

# Quantifying negative radiative forcing of non-permanent and permanent soil carbon sinks

Jens Leifeld<sup>\*</sup>, Sonja G. Keel

*Climate and Agriculture Group, Agroscope, Reckenholzstrasse 181, CH-8046 Zurich, Switzerland*

## ARTICLE INFO

Handling Editor: Budiman Minasny

### Keywords:

Soil carbon sequestration  
Impulse response function  
Carbon market  
Mitigation  
CO<sub>2</sub>

## ABSTRACT

Reversibility of soil carbon sinks is a major obstacle in assigning soil carbon sequestration as negative emission technology and it is still unclear how a non-permanent CO<sub>2</sub> removal shall be accounted for. In this study, we combine various scenarios of reversible and non-reversible soil carbon sinks with atmospheric CO<sub>2</sub> impulse response functions and calculations of the resulting radiative forcing. A time horizon of up to 500 years was considered. Results show that any soil carbon sink generates negative radiative forcing (i.e., cooling) when aggregated over longer time scales. Whereas also non-permanent CO<sub>2</sub> removals from the atmosphere provide negative average radiative forcing, their effect is substantially smaller than that of permanent removals of the same magnitude. We show that the average annual soil organic carbon balance over the integrated time window largely determines the average radiative forcing independently of rates of carbon gain or loss and longevity of the sink. This basic principle allows an unbiased assessment, comparison, and rating of mitigation projects that take advantage of soil carbon. The suggested approach is based on quantitative and relatively simple metrics and may therefore support guidance to climate policies and soil carbon markets.

## 1. Introduction

Soil organic carbon (SOC) sequestration (SCS) is considered an important building block for offsetting unavoidable anthropogenic greenhouse gas (GHG) emissions and to meet the Paris Agreement objectives (Soussana et al., 2019). The process has been defined as “transferring CO<sub>2</sub> from the atmosphere into the soil of a land unit, through plants, plant residues and other organic solids which are stored or retained in the unit as part of the soil organic matter” (Olson et al., 2014). In order to play a relevant role in mitigation, and as a negative CO<sub>2</sub> emission technology (NET), requirements for successful implementation of SCS projects or policies encompass additionality, no leakage, and permanence of the SOC store (Thamo and Pannell, 2016). Because soils are open systems, any organic molecule entering soil will eventually leave it, mostly as CO<sub>2</sub>, albeit some organic carbon may reside in the soil for centuries to millennia (e.g., Balesdent et al., 2018). Hence, permanence of soil carbon sinks is a major challenge towards contributing to climate goals and carbon offsetting and proper accounting of non-permanence seems key to a scientific sound implementation of soil carbon sinks on so-called voluntary carbon markets. Currently, the (known) non-permanence of SCS is addressed by issuing

carbon credits only for limited periods, typically 25 to 100 years as the minimum duration the offset must be maintained (Dynarski et al., 2020). Another way to address non-permanence is installing withhold buffers, i.e. the carbon credits are deducted (von Unger and Emmer, 2018). While these approaches might be deemed useful in terms of carbon finance, they are unsatisfactory from a scientific perspective. Also in climate and agricultural policies SCS, which can be considered as an inherent building block of so-called carbon farming, has been suggested as part of a solution (COWI et al., 2021), but the obstacle of how to deal with non-permanence applies to them as well. In consequence, Oldfield et al. (2022) rightly appealed for enhanced consistency among protocols of SCS in mitigation projects.

Whereas the reversibility of SCS and the implication for its role as a NET technology has been explicitly discussed in science (e.g., Bossio et al., 2020; Paustian et al., 2016; Smith, 2016), the atmospheric part of the SCS definition above has received amazingly little attention in the discussion on SOC sinks. Following small perturbations, such as transitory or permanent carbon removal or emission of moderate magnitude, atmospheric CO<sub>2</sub> concentrations tend to re-equilibrate with other earth system carbon reservoirs, i.e. oceans and the terrestrial biosphere. This re-equilibration occurs owing to the tight coupling of these reservoirs

<sup>\*</sup> Corresponding author.

E-mail addresses: [jens.leifeld@agroscope.admin.ch](mailto:jens.leifeld@agroscope.admin.ch) (J. Leifeld), [Sonja.keel@agroscope.admin.ch](mailto:Sonja.keel@agroscope.admin.ch) (S.G. Keel).

and is well studied from the absorption of large quantities of anthropogenic CO<sub>2</sub> by land and oceans (IPCC, 2021a). The temporal dynamics of atmospheric CO<sub>2</sub> following carbon removal or emission is often described by impulse response functions that represent the atmospheric CO<sub>2</sub> as consisting of multiple fractions with assigned lifetimes. The corresponding parameters are derived from complex earth system modelling (ESM) (see e.g. Gasser et al., 2017) and impulse response functions can be regarded as a simplified representation of atmospheric CO<sub>2</sub> dynamics, or that of other greenhouse gases, based on the results of ESMs. Unlike the name suggests, "impulse" functions are also suitable for representing atmospheric CO<sub>2</sub> dynamics with sustained emissions or removals (Millar et al., 2017; Smith et al., 2018). The functions describe the temporal change in atmospheric CO<sub>2</sub> content following removal or release. The parameters of these functions, together with the radiative efficiency of CO<sub>2</sub>, finally allow to calculate the instantaneous radiative forcing (RF) and the absolute global warming potential (AGWP), i.e. RF integrated over a given time period of the perturbation (Joos et al., 2013). Radiative forcing has been defined as the change in the net, downward minus upward, radiative flux (expressed in W m<sup>-2</sup>) due to a change in an external driver of climate change, such as a change in the concentration of atmospheric CO<sub>2</sub> (IPCC, 2021a). For instantaneous CO<sub>2</sub> removals or releases, the resulting RF is linearly related to the amount of CO<sub>2</sub> withdrawn from or emitted into the atmosphere. Here, CO<sub>2</sub> removals are denoted with a negative sign and result in negative RF; CO<sub>2</sub> emissions are denoted with a positive sign and result in positive RF. Hence, for the same rate of uptake or release, the absolute size of RF and AGWP resulting from changes in atmospheric CO<sub>2</sub> after instantaneous removals or releases is similar, but opposite in sign (Keller et al., 2018; Neubauer and Magonigal, 2019). Yet, quantifying the radiative forcing of reversible (i.e., loss of the formerly sequestered SOC) carbon sinks or longer lasting changes in the carbon budget is a major challenge. The time dependency of the atmospheric CO<sub>2</sub> concentration response to a perturbation implies that not only the sink size, but also the rate at which SOC is built up, or lost, as well as the duration of the sink affects RF and AGWP even if the size of the sink or source is the same.

Calculating the response of RF and AGWP to reversible soil carbon sinks allows evaluating their potential effect on the climate, also in comparison to a non-reversible SCS, i.e., a permanent sink of same magnitude. Such a calculation may thereby also provide an unbiased assessment, comparison, and rating of mitigation projects that make use of SCS. The goal of our study is to evaluate an approach that is relatively simple but at the same time provides a more mechanistic way to account for the reversibility of soil carbon sinks in the context of carbon markets as compared to current lump-sum approaches. We do this by calculating RF and AGWP time-series over 100 and 500 years for reversible and non-reversible SOC sinks of the same size that are built up and, in case of a reversible sink, degrade at different rates back to their previous SOC level. These rates translate into different periods of build-up and release and therefore different average annual SOC balances for the studied period. The targeted sink is -2 kg CO<sub>2</sub> m<sup>-2</sup>, which equals an annual sequestration of -0.027 kg SOC m<sup>-2</sup> for a duration of 20 years, in line with rates often found in agriculture (Minasny et al., 2017). The experiments are complemented by calculating the radiative effect of non-reversible CO<sub>2</sub> sources of 2 kg CO<sub>2</sub> m<sup>-2</sup>, and by looking at the radiative effect of different sink sizes.

## 2. Methods

### 2.1. Impulse response function

Instantaneous radiative forcing (RF; [W m<sup>-2</sup>]) from changes in atmospheric CO<sub>2</sub> following the change in soil C and its time-integrated value, the absolute global warming potential AGWP [W m<sup>-2</sup> a], was calculated following (Joos et al., 2013).

$$RF = (a_0 + \sum_{i=1}^3 a_i \times e^{\left(\frac{-t}{\tau_i}\right)}) \times R_E \quad (1)$$

In this approach atmospheric CO<sub>2</sub> dynamics is described by four non-interacting CO<sub>2</sub> reservoirs a<sub>0</sub>, a<sub>1</sub>, a<sub>2</sub>, a<sub>3</sub> (relative shares 0.2173; 0.224; 0.2824; 0.2763), and corresponding first-order perturbation life times τ<sub>i</sub> of ∞, 394.4, 36.54, and 4.304 years, respectively. According to Millar et al. (2017), these four reservoirs can best be understood as representing geological re-absorption, deep ocean invasion/equilibration, biospheric uptake/ocean thermocline invasion, and rapid biospheric uptake/ocean mixed-layer invasion, respectively.

Following a net CO<sub>2</sub> release from soil, each of these four reservoirs gains carbon according to its relative share. In contrast, following a net CO<sub>2</sub> uptake of the soil, each of these four reservoirs loses carbon according to its relative share. In case of a soil carbon stock in steady-state, when CO<sub>2</sub> uptake and CO<sub>2</sub> release of the soil are of equal size, the atmospheric pool is not affected.

RF was computed as the product of atmospheric CO<sub>2</sub> and its radiative efficiency R<sub>E</sub> of 1.7049<sup>-15</sup> W m<sup>-2</sup> kg CO<sub>2</sub><sup>-1</sup>. The latter represents the radiative forcing per unit change in concentration and was calculated from the radiative efficiency of CO<sub>2</sub> of 1.33 × 10<sup>-5</sup> W ppb<sup>-1</sup> (IPCC, 2021b) and a conversion to unit mass as provided by (Myhre et al., 2013) based on an atmospheric mass of 5.1352x10<sup>18</sup> kg. For simplification, we assume RF to be independent of the change of the atmospheric CO<sub>2</sub> concentration, which is reasonable for relatively small atmospheric perturbations at a given background (Myhre et al. 2013). Following Joos et al. (2013) we assume the parameters in eq. (1) to be constant. Changes in atmospheric CO<sub>2</sub> and SOC, respectively, were calculated for annual time steps.

The AGWP is then calculated as.

$$AGWP = \int_0^H RF(t)dt \quad (2)$$

with H the time horizon of the integration [years]. Dividing AGWP by H gives the average RF [W m<sup>-2</sup>]. In this study, all experiments were calculated over 500 years and results are presented for 0–100 and 0–500 years. Negative RF and AGWP denotes cooling, positive denotes warming. An uncertainty estimate for the impulse response function is provided in the Supplement.

### 2.2. Scenario experiments

We computed various simplified but realistic trajectories of reversible and non-reversible changes in SOC storage, with annual time steps, to cover a wide range of possible land management impacts on RF and AGWP. Four experiments address the relationship between the size of sinks (negative sign) and sources (positive sign), the temporal change of the soil C sink, and the resulting RF and AGWP. In these experiments 'A', 'B', 'C', and 'E' changes in SOC [kg CO<sub>2</sub> m<sup>-2</sup>] follow a trapezoidal shape with an initial 20 years lag time (no change in SOC stock), a linear SOC increase, a hold-time (no change in SOC stock), followed by a linear decrease (experiments 'A', 'B', 'E' only) back to the initial level (i.e., reversible sink). In experiment 'C' the sink is maintained once the target value is reached (i.e., permanent sink). In addition to these four set-ups, experiment 'D' quantifies the AGWP of a finite CO<sub>2</sub> source. For each experiment, different uptake and loss rates, hold-times, and magnitudes of sources and sinks were calculated to evaluate the response of RF and AGWP to differences in sink size, ramp time (in- and decrease of SOC stock), hold time, change rate, and reversibility. The set-up of the five experiments is detailed below:

- A. Sink size of a reversible sink. Increase of the SOC stock at annual rates of -0.05, -0.1, -0.15, -0.2, -0.25, -0.3, -0.35, -0.4, -0.45,

−0.5, −0.55, −0.6 kg CO<sub>2</sub> m<sup>−2</sup> over 20 years, hold time 20 years, decrease at same rates, fade out 420 years. This experiment mimics the effect of adding different amounts of organic matter to soil and stopping that practice after 20 years, thereby inducing the SOC stock to return to the pre-experimental value. The minimum and maximum sinks are 20 years × −0.05 kg CO<sub>2</sub> m<sup>−2</sup> = −1.0 kg CO<sub>2</sub> m<sup>−2</sup> and 20 years × −0.6 kg CO<sub>2</sub> m<sup>−2</sup> = −12 kg CO<sub>2</sub> m<sup>−2</sup>, respectively. For a lag time, build-up time, hold-time, and release period of 20 years each, 420 years are left over a 500 years simulation to follow the long-term change in atmospheric CO<sub>2</sub> and the corresponding effect on RF and AGWP.

- B. Temporal dynamics of a reversible sink. Twelve runs that combine ramping (years) and rate to reach a target sequestration of −2 kg CO<sub>2</sub> m<sup>−2</sup> (5 years, −0.400 kg CO<sub>2</sub> m<sup>−2</sup> a<sup>−1</sup>; 10, −0.200; 15, −0.133; 20, −0.100; 25, −0.080; 30, −0.067; 35, −0.057; 40, −0.050; 45, −0.044; 50, −0.040; 60, −0.033; 70 years, −0.029 kg CO<sub>2</sub> m<sup>−2</sup> a<sup>−1</sup>). Return to pre-experimental SOC with same ramp and rate. Fade out 320 to 450 years. The difference to experiment ‘A’ lies in the duration of build-up and release. The experiment mimics the effect of different management practices with different intrinsic rates of SOC gains and losses. Those practices with smaller intrinsic rates of SOC gain need to be practiced longer to reach the target stock.
- C. Irreversible (i.e., permanent) sink. Same ramping and rates as ‘B’, but the achieved sink of −2 kg CO<sub>2</sub> m<sup>−2</sup> becomes permanently stored in soil.
- D. Finite source. Same as ‘C’, but with opposite rate sign, representing an irreversible SOC loss of 2 kg CO<sub>2</sub> m<sup>−2</sup>.
- E. Sink duration. Ramping over 20 years with rate of −0.1 kg CO<sub>2</sub> m<sup>−2</sup> a<sup>−1</sup>, hold time 10, 20, 30, 40, 50, 75, 100, 200 years. Return to pre-experimental SOC with same rate. This experiment represents different levels of success to keep the gained carbon in soil. In practice, this could represent the amount of time a certain management is maintained.

The annual changes in SOC stocks computed in experiments ‘A’ – ‘E’, *dSOC*, are added up to provide time-integrated SOC balances *SOCint* [kg CO<sub>2</sub> m<sup>−2</sup>].

$$SOCint = \int_0^H dSOC(t)dt \quad (3)$$

with *H* the time horizon of the integration (here 100 or 500 years). The ratio of *SOCint* to *H* gives the average annual SOC balance *SOCavg* [kg CO<sub>2</sub> m<sup>−2</sup> a<sup>−1</sup>], which corresponds, in case of a permanent or temporary sink, to the average annual sink size and, in reverse, to the average annual source size in case of a permanent or temporary source. The expression *SOCavg* also allows to evaluate management effects on *RF* and *AGWP* for experiments that consecutively or alternately encompass both, sources and sinks.

### 3. Results

An illustration of a reversible SOC sink as used in experiment B is depicted in Fig. 1. The temporary uptake results in a maximum sink size of −2 kg CO<sub>2</sub> m<sup>−2</sup>, which corresponds here to long-term annual average SOC balances (*SOCavg*) of −0.79 and −0.16 kg CO<sub>2</sub> m<sup>−2</sup> a<sup>−1</sup> over 100 and 500 years, respectively (dashed lines in Fig. 1).

With different rates of CO<sub>2</sub> uptake and release back to the atmosphere, the atmospheric CO<sub>2</sub> concentration and the corresponding instantaneous radiative forcing show a typical shape that is determined by the fractional reservoirs and their perturbation lifetimes. In the case of a reversible sink (Fig. 2), the carbon uptake by soil induces an increasingly negative radiative forcing (cooling) during the period of ongoing SCS. The 20-years hold time (when CO<sub>2</sub> uptake is balanced by CO<sub>2</sub> release) leads to a weakening of the negative RF owing to the gradual replenishment of the atmospheric CO<sub>2</sub> pool from the terrestrial

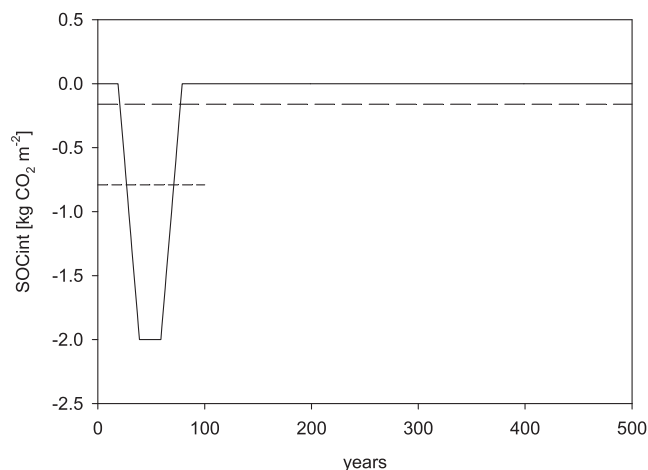


Fig. 1. Example for the build-up (20 years; C input > C loss), hold (20 years; C input = C loss) and loss (20 years; C input < C loss) of a soil carbon sink of up to −2 kg CO<sub>2</sub> m<sup>−2</sup> with 20 years initial lag time and fade-out of 420 years. The solid black line shows the time-integrated SOC balance (*SOCint*). The short dashed and long dashed lines denote the average annual SOC balances (*SOCavg*) for 100 years (−0.79 kg CO<sub>2</sub> m<sup>−2</sup>) and 500 years (−0.16 kg CO<sub>2</sub> m<sup>−2</sup>) years, respectively. The |rate| of SOC gain and loss during build-up and release is 0.1 kg CO<sub>2</sub> m<sup>−2</sup> a<sup>−1</sup>.

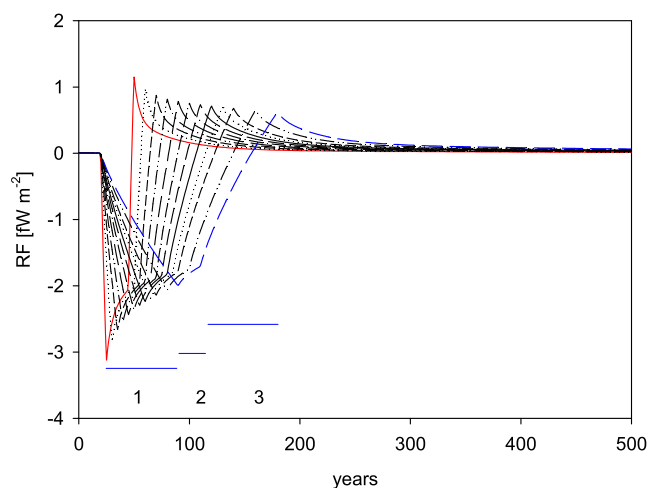


Fig. 2. Instantaneous radiative forcing (*RF*) over 500 years for a non-permanent soil carbon sink of −2 kg CO<sub>2</sub> m<sup>−2</sup> established over 5 (red), 70 (blue) years and at 10 intermediate rates (10 – 60 years, black lines) (experiment ‘B’ in methods). The sink is initialized at year 20, held for 20 years once −2 kg are reached and converted into a CO<sub>2</sub> source at the same rate thereafter to reach the pre-experimental SOC sink after 50 (red) to 180 years (blue). Horizontal bars numbered 1–3 demonstrate the periods of build-up, hold-time, and release for the low sequestration rate that is depicted by the blue line. (For interpretation of the references to colour in this figure legend, the reader is referred to the web version of this article.)

and marine reservoirs. Once the former sink is converted to a source (i.e. in practice this could mean that C inputs to the soil are reduced), *RF* becomes less negative and converts to an instantaneous warming after between 50 and 160 years that remains positive until the end of the experiment. These effects, a relative inertia of the atmospheric CO<sub>2</sub> after stopping active sequestration, and overshooting has been described before (Dommain et al., 2018; Keller et al., 2018) and can be assigned to the kinetics of the slow and fast reservoirs of the atmospheric CO<sub>2</sub> pool, respectively. The overshooting, in particular, is related to the slower uptake rate of atmospheric CO<sub>2</sub> by the terrestrial and marine reservoirs as compared to the release rate from soil.

Also in the case of a permanent sink, the active sequestration of which ends once the target value of  $-2 \text{ kg CO}_2 \text{ m}^{-2}$  is reached after between 25 and 75 years, the maximum negative RF turns back to smaller values, but remains negative throughout the course of the experiment (Fig. 3). In both cases, the RF time-course of the twelve runs reflects the order of  $\text{CO}_2$  uptake and release rates.

Whereas the instantaneous RF describes the radiative effect at any single point in time, its time integral AGWP, which is also used to calculate global warming potentials of different greenhouse gases, is a more meaningful measure for the comparison of scenarios. Sequestering SOC over 5 to 70 years at different rates to reach the targeted sink of  $-2 \text{ kg CO}_2 \text{ m}^{-2}$  generates a negative AGWP (i.e., a cooling) during build-up (upper bundle in Fig. 4). With slower build-up of the sink (blue line), AGWP becomes more negative than with fast build-up (red line). After the peak sink has been reached, a 20-years hold time follows before the sink is reversed. Maximum negative AGWP is reached after between 50 years (fast build-up) and 157 years (slow build-up). After that maximum, AGWP becomes less negative over time, induced by the atmospheric response to the  $\text{CO}_2$  withdrawal. Yet, even after 500 years, AGWP remains negative in all calculations (upper bundle in Fig. 4). For a permanent sink (lower bundle in Fig. 4), i.e. holding the achieved  $-2 \text{ kg CO}_2 \text{ m}^{-2}$  during the whole experiment, the AGWP demonstrates steadily increasing negative forcing far beyond the period of actual SCS. The ratio of AGWP's between a non-permanent and a permanent sink reveals that the cooling effect of the first is much smaller but still 4 to 16 % of that of a permanent sink after 500 years (green lines in Fig. 4).

The average RF over 100 and 500 years depends almost linearly on the average annual SOC balance (i.e. net gain or loss) over the integrated time window across the wide range of SOC build-up and loss scenarios (Fig. 5). For example, an average annual SOC balance of  $-1 \text{ kg CO}_2$  converts into a mean negative forcing of  $-0.90$  (100 years) and  $-0.62 \text{ fW m}^{-2}$  (500 years) (100 years - black and grey line in Fig. 5; 500 years - blue line in Fig. 5, respectively), thereby providing a suitable proxy for assessing the climate effect of any kind of soil C sink. Because AGWP is average RF times the time horizon of integration, H, also AGWP is an almost linear function of the average annual SOC balance (Fig. 6).

Results in Table 1 use this relationship and compare the effect of creating a temporary SOC sink of variable duration relative to a permanent sink of the same size. These scenarios (1–5) are not explicitly part of the experiments 'A'–'E', but represent different hold-times as also used for experiment 'E'. However, compared to 'E', no lag-time is used

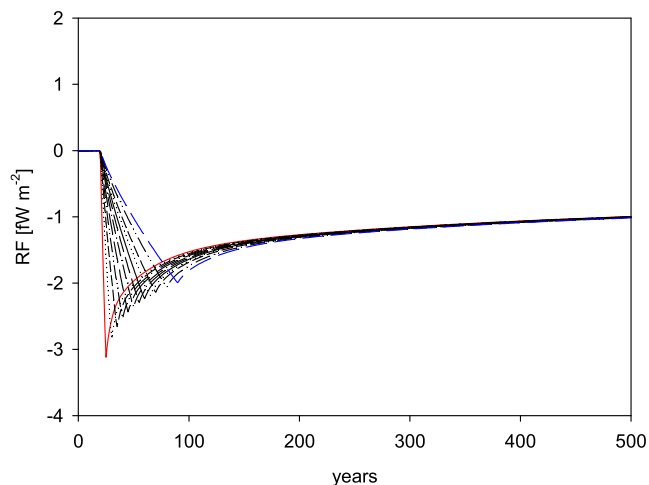


**Fig. 3.** Instantaneous radiative forcing (RF) over 500 years for a permanent soil carbon sink of  $-2 \text{ kg CO}_2 \text{ m}^{-2}$  established over 5 (red), 70 (blue) years and at 10 intermediate rates (10–60 years, black lines) (experiment 'C' in methods). The sink is initialized at year 20 and maintained once the maximum is reached. (For interpretation of the references to colour in this figure legend, the reader is referred to the web version of this article.)

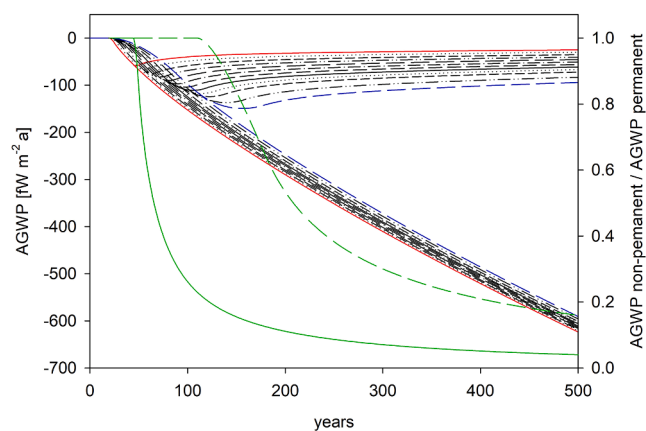


**Fig. 4.** Absolute global warming potential (AGWP) over 500 years for a non-permanent (upper bundle of lines; experiment 'B' in methods) and a permanent (decreasing bundle of lines; experiment 'C' in methods) soil carbon sink of  $-2 \text{ kg CO}_2 \text{ m}^{-2}$  established over 5 (red), 70 (blue) years and at 10 intermediate rates (10–60 years, black lines). In both experiments, the sink is initialized at year 20, held for only 20 years and converted into a  $\text{CO}_2$  source at same rates thereafter in the case of non-permanence to reach the pre-experimental SOC stock after 50 (red) to 180 years (blue). Green lines show the ratio of AGWP non-permanent to AGWP permanent for the experiments with 5 (solid) and 70 (dashed) years of sequestration. (For interpretation of the references to colour in this figure legend, the reader is referred to the web version of this article.)

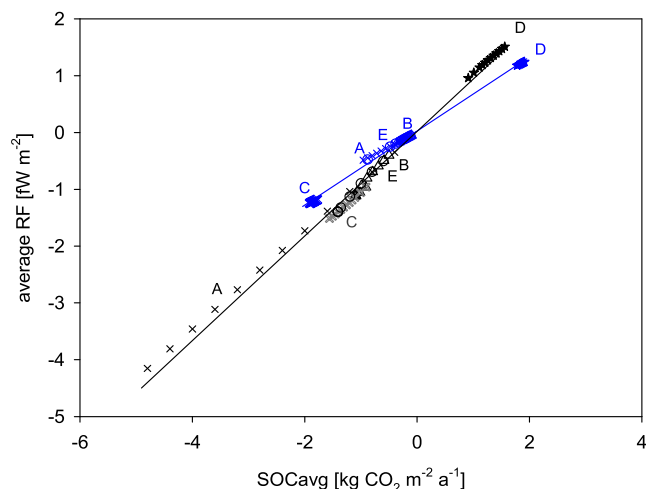


**Fig. 5.** Relationship between average annual SOC balance (SOCavg) and average radiative forcing (RF) over 100 (black, grey) and 500 (blue) years for all calculations. Letters refer to the five experiments (see methods) with symbols representing the individual units (i.e., rates, hold-times, size). Linear regression coefficients  $y = a + b \cdot x$  with  $a$  and  $b = 0.0139$  and  $0.9150$  (100 years) and  $0.0285$  and  $0.6503$  (500) years, respectively.  $R^2 > 0.99$  in both cases. The total number of (sub)experiments is 56. (For interpretation of the references to colour in this figure legend, the reader is referred to the web version of this article.)

and a time horizon of only one century is applied. The scenarios in Table 1 exemplify that, over 100 years, a non-permanent sink of  $-2 \text{ kg CO}_2 \text{ m}^{-2}$  that is built-up over 20 years, held for 20 years and lost over the following 20 years, achieves a cooling of almost 44 % of that of the permanent sink. Correspondingly, longer hold-times reach higher negative forcing.

The close, linear relationship between the average annual SOC balance and both RF and AGWP implies that atmospheric  $\text{CO}_2$  changes in a predictable manner and in accordance with SOC for any given scenario experiment and time horizon. Fig. 7 illustrates the relationship between

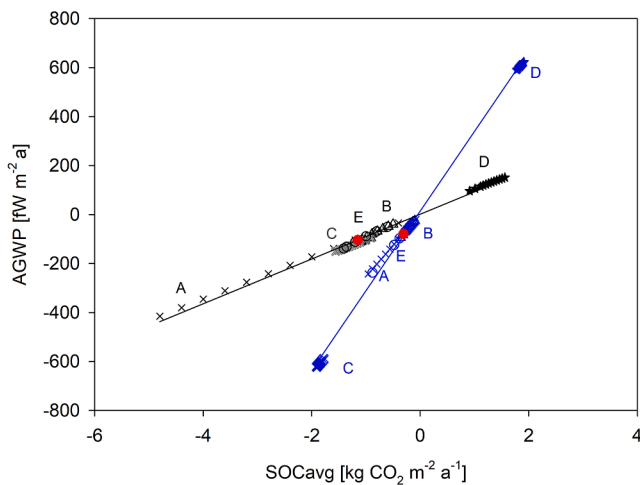


**Fig. 6.** Relationship between average annual SOC balance (SOCavg) and absolute global warming potential (AGWP) over 100 (black, grey) and 500 (blue) years for all calculations. Letters refer to the five experiments (see methods) with symbols representing the individual units (i.e., rates, hold-times, size). Linear regression coefficients  $y = a + b \cdot x$  with  $a$  and  $b = 1.386$  and  $91.495$  (100 years) and  $14.25$  and  $325.17$  (500 years), respectively.  $R^2 > 0.99$  in both cases. The total number of (sub)experiments is 56. (For interpretation of the references to colour in this figure legend, the reader is referred to the web version of this article.)

**Table 1**

Average annual SOC balance (SOCavg) and corresponding average radiative forcing RF for different hold-times of the sink, calculated based on parameters in Fig. 5 for a 100-year time horizon. The first four scenarios are: Instantaneous SOC sequestration (i.e., no lag time) at rate of  $-0.1 \text{ kg CO}_2 \text{ m}^{-2} \text{ a}^{-1}$  for 20 years, hold-time (time during which  $\text{CO}_2$  uptake and release are equal) at  $-2 \text{ kg CO}_2 \text{ m}^{-2}$  for 20, 30, 40, 50 years, followed by SOC loss of  $0.1 \text{ kg CO}_2 \text{ m}^{-2} \text{ a}^{-1}$  to reach the pre-experimental SOC stock after 60, 70, 80, and 90 years, respectively. Scenario five denotes a permanent sink of  $-2 \text{ kg CO}_2 \text{ m}^{-2}$  with same build-up as scenarios 1–4.

Scenario	Hold time [years]	SOCavg [ $\text{kg CO}_2 \text{ m}^{-2} \text{ a}$ ]	average RF [ $\text{fW m}^{-2}$ ]	% RF of permanent sink
1	20	-0.80	-0.718	43.7
2	30	-1.00	-0.901	54.9
3	40	-1.20	-1.084	66.0
4	50	-1.40	-1.267	77.2
5	100	-1.81	-1.642	100

the average SOC balance and the resulting change in atmospheric  $\text{CO}_2$ . For a period of one century, an average annual SOC balance of one  $\text{kg CO}_2$  results in a change of  $0.53 \text{ kg}$  ( $0.37 \text{ kg}$  for 500 years) in atmospheric  $\text{CO}_2$ .

## 4. Discussion

### 4.1. Method discussion

In this study SOC sequestration was depicted in simple but quantitatively realistic scenarios in order to cover various possible pathways of build-up and eventual release. We chose this approach to produce results, which follow a systematic design, are transparent, and are useful to e.g. represent effects of different agricultural management practices. Although temporal SOC dynamics as revealed from process-based modelling or long-term field observations can be more complex (Johnston et al., 2009), the relationships described in Figs. 5 and 6 are also applicable to those types of SOC time-series. The atmospheric part of the calculations is based on applying impulse response functions; an approach that has been followed frequently (Allen et al., 2018; Boucher

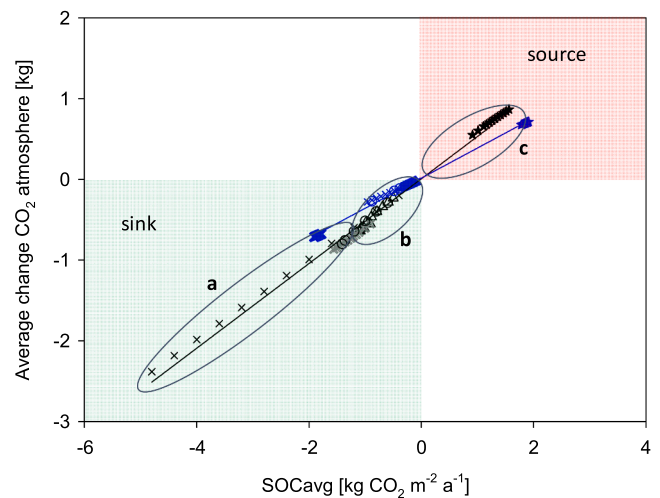


**Fig. 7.** Relationship between average annual SOC balance (SOCavg) and average change in atmospheric  $\text{CO}_2$  over the same time period for a time horizon of 100 (black, grey) and 500 (blue) years. The conversion factor from soil C to atmosphere C is  $0.53$  and  $0.37$  for 100 and 500 years, respectively. The three ellipsoids (a, b, c) denote the typical range of permanent sinks, reversible sinks, and irreversible sources, respectively. (For interpretation of the references to colour in this figure legend, the reader is referred to the web version of this article.)

et al., 2009; Keller et al., 2018; Millar et al., 2017). It can be considered as a surrogate to the description of multidimensional atmospheric feedbacks to disturbances, as revealed from earth system modelling, in more simple terms. The parameterization used here is based on Joos et al. (2013), with the radiative efficiency of  $\text{CO}_2$  taken from (IPCC, 2021b). It must be noted that the radiative efficiency depends on the overall atmospheric  $\text{CO}_2$  concentration (Myhre et al., 2013), and the chosen value represents the current-day situation. Yet, it allows comparing different sequestration scenarios as computed in this study. Other parameterizations regarding the distribution of atmospheric  $\text{CO}_2$  among reservoirs have been applied for studying the forcing effect of more longer-lived soil carbon pools such as in peatlands accumulating carbon over millennia (Dommain et al., 2018). Whereas the obtained RF time-courses slightly differ depending on the chosen parameterization, the observed patterns (inertia, overshooting) do not. In addition, it is known that the climate effect of SCS is not only related to the corresponding  $\text{CO}_2$  balance, but also to eventual changes in the net fluxes of other soil-born greenhouse gases, namely  $\text{N}_2\text{O}$  and  $\text{CH}_4$ . These were not considered in the example calculations, but may become relevant in the case of actual implementation (e.g. Guenet et al., 2021).

### 4.2. Radiative forcing of soil carbon sequestration

Our analysis reveals that i) the change in radiative forcing as induced by a soil carbon sink is physically related to the sink size and ii) permanence is an important attribute of a soil carbon sink to provide an effective mitigation measure (with ‘permanence’ referring here to remaining stable over the simulation period, not in absolute terms). The longer the time integration is, the more important permanence becomes. For a permanent sink both RF and AGWP are constantly negative throughout the simulation period of 500 years, despite the partial re-equilibration of the atmospheric  $\text{CO}_2$  pool. However, also full reversal of a soil carbon sink delivers a climate benefit as compared to creating no sink at all. As examples in Table 1 show, non-permanent sinks can make a significant contribution to climate cooling also relative to a permanent sink over the course of one century.

Yet, how much of the potential of a permanent sink can be realized by a reversible one depends on the integration period as well as on the rates of SOC accumulation and release, and duration of hold time (phase

during which CO<sub>2</sub> uptake and release are in balance). In all simulations the time-courses of IF and AGWP are complex and may become even more so when not trapezoidal but non-linear functions for SOC accumulation and release were chosen. Therefore, and in order to provide a metric that is also useful for the accounting of any type of non-permanent and permanent SOC sinks, the relationship we describe between mean RF or AGWP, respectively, and average annual soil carbon balance as depicted in Figs. 5 and 6 is an important step to reaching this goal.

Results in Figs. 5 and 6 suggest that the average annual SOC balance determines the mean RF and the AGWP. It also determines the ratio of the average sink to the change in atmospheric CO<sub>2</sub> of any type of studied sink-source relationship (Fig. 7). The reversibility of SOC sinks is widely acknowledged as inherent to soil and has been a point for discussion in the context of climate smart agriculture and the contribution of SCS to reaching climate goals, and maybe more importantly, in the development of carbon markets with their attempt to offset fossil emissions (von Unger and Emmer, 2018). While the latter, once avoided, can be accounted for as savings, the reversibility of sinks remains a caveat to their proper quantitative assessment and successful implementation. Current sink project regulations require monitoring and verifying the SOC stocks on regular basis (Aynekulu et al., 2011; GoldStandard, 2020; VCS, 2011). This may be achieved also by combination of methods (Smith et al., 2020). Whereas SOC monitoring is also necessary when quantification of the corresponding RF and AGWP is sought for, findings in Figs. 5–7 allow a quantitative comparison and rating of different projects or measures among each other, based on their climate forcing. Further they are able to account for the fact that mineral soil is not an infinite sink, but tends to reach new SOC equilibrium after some decades (Paustian et al., 2016). For example, how a temporary sink of  $-2 \text{ kg CO}_2 \text{ m}^{-2}$  that is built-up over 20 years (no lag time), held for 20 years and then lost over the following 20 years, can be rated against a longer-lived sink of 30 years and a permanent one both of the same size can be assessed with this approach. Such scenarios would apply, for example, to sequestration measures like the introduction of cover crops with return to the previous management after 20 or 30 years as compared to keeping them as part of a climate smart agriculture. As Table 1 shows, the shorter-lived sink is, over 100 years, worth 44% of the permanent one, and a medium-lived sink of 30 years is 55% that of a permanent one. Hence, the longevity of a sink is an important factor for its climate effect.

The cooling effect of reversible carbon sinks in terrestrial ecosystems has been previously studied by Matthews et al. (2022) and Sierra et al. (2021). Matthews et al. (2022) investigated how an enhancement of terrestrial carbon storage in plants over the next several decades changes global temperature when returned to the atmosphere during the second half of this century, using a global climate model of intermediate complexity. They underpinned that also temporary sinks can make an important contribution, albeit global climate goals were only achievable with strong reductions in fossil CO<sub>2</sub> emissions. Furthermore, these authors stressed that the temperature effect would be dampened by a reduced surface albedo in case carbon sinks were generated by afforestation. Also biochar application to soil, a promising NET and SCS measure (Lehmann et al., 2021) may reduce surface albedo, although this effect might be short-lived owing to the incorporation of the black material into the soil matrix over time (Genesio et al., 2012). Sierra et al. (2021) analysed the climate benefit of carbon sequestration using an ecosystem carbon model in combination with impulse response functions similar to those used in this study. They defined carbon sequestration as the fate of a certain amount of carbon taken up by the sequestering system at a time and its transit time before re-entering the atmosphere. They highlighted the important role of the transit time of carbon, i.e. the time it takes the carbon to traverse the system: Increasing the transit time was, in addition to increasing inputs, regarded as key to achieve a climate benefit from sequestration. The simplified approach we suggest here can easily be implemented for carbon accounting. Its results are in line with important findings of previous studies, but

focuses on deriving the radiative forcing just from changing SOC stocks over time without the need of knowing input rates, transit times, or running model simulations.

#### 4.3. Soil carbon sequestration and its radiative effect at global scale

Our results essentially refer to SOC gains as observed in mineral soils. In the example calculations, the average instantaneous RF over 100 years for a build-up time of 20 years (i.e.,  $-0.1 \text{ kg CO}_2 \text{ m}^{-2} \text{ a}^{-1}$ ) and an initial lag phase of 20 years is  $-0.69$  and  $-1.39 \text{ fW m}^{-2}$  for a reversible and non-reversible sink, respectively. Deploying these values to the world's cropland area (1594 Mha excluding high SOC and sandy soils; Zomer et al., 2017) reveals an overall RF of  $-0.011$  and  $-0.022 \text{ W m}^{-2}$ , respectively. These effect sizes are c. one order of magnitude smaller than those estimated for large-scale peatland rewetting on a much smaller area (Günther et al., 2020; Ojanen and Minkkinen, 2020). In terms of radiative forcing, rewetting of organic soils differs in two respects from SCS in mineral soils. The climate benefit of peatland rewetting is mostly induced by avoided CO<sub>2</sub> emissions. This effect is considered to work immediately after raising the water table (Wilson et al., 2016). More importantly, the effect is long-lasting as all peat, that would oxidize under drained conditions, becomes protected by rewetting. The size of this protectable carbon pool is in the order of 1600 t SOC ha<sup>-1</sup> or 80.8 Gt SOC globally (Leifeld and Menichetti, 2018) as compared to a sink size in mineral soil of  $-2 \text{ kg CO}_2 \text{ m}^{-2}$  as in the example above, which corresponds to 8.7 Gt SOC for 1594 Mha.

A mineral soil carbon increase from a sink of  $-2 \text{ kg CO}_2 \text{ m}^{-2}$  on all cropland equals  $0.43 \text{ Pg C a}^{-1}$  over 20 years, or 3.3 ‰ of the world's cropland SOC stock of 132 Pg C in 0 – 0.3 m (Zomer et al., 2017, excluding high SOC and sandy soils). This is close to the aspirational goal of the 4 per 1000 initiative, launched at the 21st Conference of Parties of the United Nations Framework Convention on Climate Change in Paris in 2015 (Rumpel et al., 2020) and underpins that the scenarios provided in this paper are within a realistic range.

## 5. Conclusions

In this study we evaluated a relatively simple approach to better account for the reversibility of soil carbon sinks in the context of the evolving carbon markets and in the light of an increasing demand for nature based solutions (Yanai et al., 2020). This approach is based on the premise that often only low-frequency SOC stock measurements will be available that nevertheless provide the basis for possible remuneration in result-based incentives (COWI et al., 2021). We show that with the time-course of SOC stocks at hand, reliable estimates of the climate benefit of reversible and permanent SCS can be deduced.

We highlight three important findings from this study:

- Not only permanent but also reversible soil carbon sinks provide a climate benefit
- The climate benefit is proportional to the average soil organic carbon balance
- A meaningful evaluation of the climate benefit includes specification of the corresponding time horizon of the measure

The presented relationships cannot replace but rather complement measurements of soil organic carbon. Together, this will provide opportunities for faster implementation of science-driven evaluation of permanent and non-permanent soil carbon sinks in terms of their effect on climate and allow a more rigid assessment of mitigation potentials by SCS (Rodrigues et al., 2021). Repeated quantification of soil carbon stocks is still essential in order to obtain average annual SOC balances, which are necessary to apply the proposed relationship between this metric and climate forcing. Recent developments in field spectroscopy (Angelopoulou et al., 2020; Viscarra Rossel et al., 2017) will help to weaken the barrier of classical resource-intensive repeated soil

inventories. In practice, our approach allows to provide guidance towards the further development of carbon markets or compensation of farmers, inform actors at project level, and facilitate SCS to become an important element of nationally determined contributions as part of the Paris Agreement framework.

### Declaration of Competing Interest

The authors declare that they have no known competing financial interests or personal relationships that could have appeared to influence the work reported in this paper.

### Appendix A. Supplementary data

Supplementary data to this article can be found online at <https://doi.org/10.1016/j.geoderma.2022.115971>.

### References

- Allen, M.R., Shine, K.P., Fuglestedt, J.S., Millar, R.J., Cain, M., Frame, D.J., Macey, A. H., 2018. A solution to the misrepresentations of CO<sub>2</sub>-equivalent emissions of short-lived climate pollutants under ambitious mitigation. *NPJ Clim. Atmos. Sci.* 1 (1), 16.
- Angelopoulos, T., Balafoutis, A., Zalidis, G., Bochtis, D., 2020. From laboratory to proximal sensing spectroscopy for soil organic carbon estimation—a review. *Sustainability* 12 (2), 443.
- Aynekulu, E., Vagen, T.-G., Shephard, K., Winowiecki, L., 2011. A protocol for modeling, measurement and monitoring soil carbon stocks in agricultural landscapes. Version 1.1., World Agroforestry Centre, Nairobi.
- Balesdent, J., Basile-Doelsch, I., Chadouef, J., Cornu, S., Derrien, D., Fekiacova, Z., Hatté, C., 2018. Atmosphere–soil carbon transfer as a function of soil depth. *Nature* 559 (7715), 599–602.
- Bossio, D.A., Cook-Patton, S.C., Ellis, P.W., Fargione, J., Sanderman, J., Smith, P., Wood, S., Zomer, R.J., von Unger, M., Emmer, I.M., Griscom, B.W., 2020. The role of soil carbon in natural climate solutions. *Nat. Sustainability* 3 (5), 391–398.
- Boucher, O., Friedlingstein, P., Collins, B., Shine, K.P., 2009. The indirect global warming potential and global temperature change potential due to methane oxidation. *Environ. Res. Lett.* 4 (4), 044007.
- COWI, Ecologic Institute, IEEP, 2021. Technical Guidance Handbook - setting up and implementing result-based carbon farming mechanisms in the EU.
- Dommain, R., Frohling, S., Jeltsch-Thömmes, A., Joos, F., Couwenberg, J., Glaser, P.H., 2018. A radiative forcing analysis of tropical peatlands before and after their conversion to agricultural plantations. *Glob. Change Biol.* 24 (11), 5518–5533.
- Dynarski, K.A., Bossio, D.A., Scow, K.M., 2020. Dynamic stability of soil carbon: reassessing the “permanence” of soil carbon sequestration. *Front. Environ. Sci.* 8 (218).
- Gasser, T., Peters, G.P., Fuglestedt, J.S., Collins, W.J., Shindell, D.T., Ciais, P., 2017. Accounting for the climate–carbon feedback in emission metrics. *Earth Syst. Dynam.* 8 (2), 235–253.
- Genesio, L., Miglietta, F., Lugato, E., Baronti, S., Pieri, M., Vaccari, F.P., 2012. Surface albedo following biochar application in durum wheat. *Environ. Res. Lett.* 7 (1), 014025.
- GoldStandard, 2020. Soil organic carbon framework methodology.
- Guenet, B., Gabrielle, B., Chenu, C., Arrouays, D., Balesdent, J., Bernoux, M., Bruni, E., Calliman, J.-P., Cardinael, R., Chen, S., Ciais, P., Desbois, D., Fouché, J., Frank, S., Henault, C., Lugato, E., Naipal, V., Nesme, T., Obersteiner, M., Pellerin, S., Powelson, D.S., Rasse, D.P., Rees, F., Soussana, J.-F., Su, Y., Tian, H., Valin, H., Zhou, F., 2021. Can N<sub>2</sub>O emissions offset the benefits from soil organic carbon storage? *Glob. Change Biol.* 27 (2), 237–256.
- Günther, A., Barthelmes, A., Huth, V., Joosten, H., Jurasinski, G., Koesch, F., Couwenberg, J., 2020. Prompt rewetting of drained peatlands reduces climate warming despite methane emissions. *Nat. Commun.* 11 (1), 1644.
- Ipc, 2021a. Annex VII: Glossary. In: Matthews, J.B.R., Möller, V., van Diemen, R., Fuglestedt, J.S., Masson-Delmotte, V., Mendez, C., Semenov, S., Reisinger, A. (Eds.), *Climate Change 2021: The physical science basis. Contribution of working group I to the Sixth Assessment Report of the Intergovernmental Panel on Climate Change*. Cambridge University Press, in press.
- IPCC, 2021b. *Climate Change 2021: The Physical Science Basis. Contribution of Working Group I to the Sixth Assessment Report of the Intergovernmental Panel on Climate Change*.
- Johnston, A.E., Poulton, P.R., Coleman, K., 2009. Soil organic matter: Its importance in sustainable agriculture and carbon dioxide fluxes. In: D.L. Sparks (Ed.), *Advances in Agronomy*, Vol 101. *Advances in Agronomy*, pp. 1–57.
- Joos, F., Roth, R., Fuglestedt, J.S., Peters, G.P., Enting, I.G., von Bloh, W., Brovkin, V., Burke, E.J., Eby, M., Edwards, N.R., Friedrich, T., Frölicher, T.L., Halloran, P.R., Holden, P.B., Jones, C., Kleinen, T., Mackenzie, F.T., Matsumoto, K., Meinshausen, M., Plattner, G.K., Reisinger, A., Segschneider, J., Shaffer, G., Steinacher, M., Strassmann, K., Tanaka, K., Timmermann, A., Weaver, A.J., 2013. Carbon dioxide and climate impulse response functions for the computation of greenhouse gas metrics: a multi-model analysis. *Atmos. Chem. Phys.* 13 (5), 2793–2825.
- Keller, D.P., Lenton, A., Scott, V., Vaughan, N.E., Bauer, N., Ji, D., Jones, C.D., Kravitz, B., Muri, H., Zickfeld, K., 2018. The carbon dioxide removal model intercomparison project (CDRMP): rationale and experimental protocol for CMIP6. *Geosci. Model Dev.* 11 (3), 1133–1160.
- Lehmann, J., Cowie, A., Masiello, C.A., Kammann, C., Woolf, D., Amonette, J.E., Cayuela, M.L., Camps-Arbestain, M., Whitman, T., 2021. Biochar in climate change mitigation. *Nat. Geosci.* 14 (12), 883–892.
- Leifeld, J., Menichetti, L., 2018. The underappreciated potential of peatlands in global climate change mitigation strategies. *Nat. Commun.* 9 (1), 1071.
- Matthews, H.D., Zickfeld, K., Dickau, M., MacIsaac, A.J., Mathesius, S., Nzotungicimpaye, C.-M., Luers, A., 2022. Temporary nature-based carbon removal can lower peak warming in a well-below 2°C scenario. *Commun. Earth Environ.* 3 (1), 65.
- Millar, R.J., Nicholls, Z.R., Friedlingstein, P., Allen, M.R., 2017. A modified impulse-response representation of the global near-surface air temperature and atmospheric concentration response to carbon dioxide emissions. *Atmos. Chem. Phys.* 17 (11), 7213–7228.
- Minasny, B., Malone, B.P., McBratney, A.B., Angers, D.A., Arrouays, D., Chambers, A., Chaplot, V., Chen, Z.-S., Cheng, K., Das, B.S., Field, D.J., Gimona, A., Hedley, C.B., Hong, S.Y., Mandal, B., Marchant, B.P., Martin, M., McConkey, B.G., Mulder, V.L., O'Rourke, S., Richer-de-Forges, A.C., Odeh, I., Padarian, J., Paustian, K., Pan, G., Poggio, L., Savin, I., Stolbovoy, V., Stockmann, U., Sulaeman, Y., Tsui, C.-C., Vågen, T.-G., van Wesemael, B., Winowiecki, L., 2017. Soil carbon 4 per mille. *Geoderma* 292, 59–86.
- Myhre, G., Shindell, D., Bréon, F.-M., Collins, W., Fuglestedt, J., Huang, J., Koch, D., Lamarque, J.-F., Lee, D., Mendoza, B., Nakajima, T., Robock, A., Stephens, G., Takemura, T., Zhang, H., 2013. *Anthropogenic and natural radiative forcing*, Cambridge.
- Neubauer, S.C., Magonigal, J.P., 2019. Correction to: Moving beyond global warming potentials to quantify the climatic role of ecosystems. *Ecosystems* 22 (8), 1931–1932.
- Ojanen, P., Minkkinen, K., 2020. Rewetting offers rapid climate benefits for tropical and agricultural peatlands but not for forestry-drained peatlands. *Global Biogeochem. Cycles* 34 (7) e2019GB006503.
- Oldfield, E.E., Eagle, A.J., Rubin, R.L., Rudek, J., Sanderman, J., Gordon, D.R., 2022. Crediting agricultural soil carbon sequestration. *Science* 375 (6586), 1222–1225.
- Olson, K.R., Al-Kaisi, M.M., Lal, R., Lowery, B., 2014. Experimental consideration, treatments, and methods in determining soil organic carbon sequestration rates. *Soil Sci. Soc. Am. J.* 78 (2), 348–360.
- Paustian, K., Lehmann, J., Ogle, S., Reay, D., Robertson, G.P., Smith, P., 2016. Climate-smart soils. *Nature* 532 (7597), 49–57.
- Rodrigues, L., Hardy, B., Huyghebaert, B., Fohrafellner, J., Fornara, D., Barančíková, G., Bárcena, T.G., De Boever, M., Di Bene, C., Feizienė, D., Kätterer, T., Laszlo, P., O'Sullivan, L., Seitz, D., Leifeld, J., 2021. Achievable agricultural soil carbon sequestration across Europe from country-specific estimates. *Glob. Change Biol.* 27 (24), 6363–6380.
- Rumpel, C., Amiraslani, F., Chenu, C., Garcia Cardenas, M., Kaonga, M., Koutika, L.-S., Ladha, J., Madari, B., Shirato, Y., Smith, P., Soudi, B., Soussana, J.-F., Whitehead, D., Wollenberg, E., 2020. The 4p1000 initiative: Opportunities, limitations and challenges for implementing soil organic carbon sequestration as a sustainable development strategy. *Ambio* 49 (1), 350–360.
- Sierra, C.A., Crow, S.E., Heimann, M., Metzler, H., Schulze, E.D., 2021. The climate benefit of carbon sequestration. *Biogeosciences* 18 (3), 1029–1048.
- Smith, C.J., Forster, P.M., Allen, M., Leach, N., Millar, R.J., Passerello, G.A., Regayre, L.A., 2018. FAIR v1.3: a simple emissions-based impulse response and carbon cycle model. *Geosci. Model Dev.* 11 (6), 2273–2297.
- Smith, P., 2016. Soil carbon sequestration and biochar as negative emission technologies. *Glob. Change Biol.* 22 (3), 1315–1324.
- Smith, P., Soussana, J.-F., Angers, D., Schipper, L., Chenu, C., Rasse, D.P., Batjes, N.H., van Egmond, F., McNeill, S., Kuhnert, M., Arias-Navarro, C., Olesen, J.E., Chirinda, N., Fornara, D., Wollenberg, E., Álvaro-Fuentes, J., Sanz-Cobena, A., Klump, K., 2020. How to measure, report and verify soil carbon change to realize the potential of soil carbon sequestration for atmospheric greenhouse gas removal. *Glob. Change Biol.* 26 (1), 219–241.
- Soussana, J.-F., Luffalla, S., Ehrhardt, F., Rosenstock, T., Lamanna, C., Havlík, P., Richards, M., Wollenberg, E., Chotte, J.-L., Torquebiau, E., Ciais, P., Smith, P., Lal, R., 2019. Matching policy and science: Rationale for the ‘4 per 1000 - soils for food security and climate’ initiative. *Soil Tillage Res.* 188, 3–15.
- Thamo, T., Pannell, D.J., 2016. Challenges in developing effective policy for soil carbon sequestration: perspectives on additionality, leakage, and permanence. *Climate Policy* 16 (8), 973–992.
- VCS, 2011. Module VMD0021 Estimation of stock in the soil carbon pool, Voluntary Carbon Standard.
- Viscarra Rossel, R.A., Lobsey, C.R., Sharman, C., Flick, P., McLachlan, G., 2017. Novel proximal sensing for monitoring soil organic C stocks and condition. *Environ. Sci. Technol.* 51 (10), 5630–5641.
- von Unger, M., Emmer, I., 2018. Carbon market incentives to conserve, restore and enhance soil carbon, Alameda, USA.

- Wilson, D., Blain, D., Couwenberg, J., Evans, C.D., Murdiyarso, D., Page, S.E., Renou-Wilson, F., Rieley, J.O., Sirin, A., Strack, M., Tuittila, E.-S., 2016. Greenhouse gas emission factors associated with rewetting of organic soils. *Mire Peat* 17, 4.
- Yanai, R.D., Wayson, C., Lee, D., Espejo, A.B., Campbell, J.L., Green, M.B., Zekwurt, J. M., Yoffe, S.B., Aukema, J.E., Lister, A.J., Kirchner, J.W., Gamarra, J.G.P., 2020. Improving uncertainty in forest carbon accounting for REDD+ mitigation efforts. *Environ. Res. Lett.* 15 (12), 124002.
- Zomer, R.J., Bossio, D.A., Sommer, R., Verchot, L.V., 2017. Global sequestration potential of increased organic carbon in cropland soils. *Sci. Rep.* 7 (1), 15554.